

# Studies on Photocatalytic Degradation of Acridine Orange and Chloroform Sensing Using as-Grown Antimony Oxide Microstructures

Aslam Jamal\*, Mohammed Muzibur Rahman, Mohammed Faisal, Sher Bahadar Khan

Centre for Advanced Materials and Nano-Engineering (CAMNE) and Department of Chemistry, Faculty of Sciences and Arts, Najran University, Najran, Kingdom of Saudi Arabia.  
Email: draslamjamal@gmail.com

Received December 7<sup>th</sup>, 2010; revised December 30<sup>th</sup>, 2010; accepted May 18<sup>th</sup>, 2011.

## ABSTRACT

Flower shaped antimony oxide ( $Sb_2O_3$ ) microstructures were synthesized in a large quantity via simple solution method using aqueous mixtures of antimony chloride and hexamethylene diamine (HMDA). The morphological characterizations were done by field emission scanning electron microscopy (FESEM), which revealed that the synthesized products possess flower-shaped microstructures. The detailed structural characterizations performed by X-ray diffraction (XRD), Fourier transform infrared spectrophotometer (FT-IR) and Raman spectrophotometer confirmed that the synthesized microstructures are well-crystalline antimony oxide. The Energy dispersive spectroscopy (EDS) shows that the grown products are composed of Sb and O. Optical properties of the synthesized products were characterized by UV-Visible spectrophotometer which exhibits a well defined peak at  $\sim 291.0$  nm. The photo-catalytic activity of the  $Sb_2O_3$  microstructures was evaluated by degradation of acridine orange (AO), which mineralized almost 63.0% in 150 min. The chemical sensing properties of  $Sb_2O_3$  microstructures was also studied by I-V technique using chloroform as a detecting solvent. The fabricated chloroform sensor demonstrates good sensitivity of  $0.1154 \mu A \cdot cm^{-2} \cdot mM^{-1}$ , lower-detection limit ( $\sim 0.1$  mM), large-linear dynamic range (LDR, 0.122 mM to 1.22 M) with linearity ( $R = 0.7898$ ) in short response time (10.0 sec).

**Keywords:** Antimony Oxide Microstructures, XRD, FE-SEM, Photo Degradation, Acridine Orange, Chloroform Chemical Sensing

## 1. Introduction

Developing nano-science and nanotechnology is getting valuable attention in terms of research and development at the present time. In the field of nanotechnology, the antimony oxide nano-crystalline particles emerges as a challenging prospect due to having amazing preparation, characterization, catalytic degradation, and fabrication as well as their wide range of other applications. The synthesis of nano-materials has received remarkable attention in view of the size, shape, structural arrangement, properties and potential applications in advance level. Generally,  $Sb_2O_3$  is used as conductive materials, high-efficiency flame-retardant synergist in polymers, dyes, pigments, paints, adhesives, and industrial coating materials [1-3].  $Sb_2O_3$  nano-rods, nano-particles, nano-tubes, nano-belts [4-6] and hollow spheres [7] have been fabricated by various conventional routes and techniques.

Micro-structured antimony oxides can be prepared by various general methods including vapor-solid route [8], hydrothermal synthesis [9,10], vapor condensation [10, 11], sol-gel [12], X-ray radiation-oxidization route [13], and gas condensation [14] techniques. However, scientist are quite interested on controlled growth, mechanism, characteristics, and advanced applications of the  $Sb_2O_3$  microstructure [15]. During the past decades, many researchers have put focus on searching for a direct and effective method to solve this problem [16,17]. Recently, the opt-electronic and surface properties of  $Sb_2O_3$  microstructures have been extensively studied [2,3]. Here we further investigate their property as a photo-catalyst and chemi-sensor.

Organic dyes such as acridine orange are the common pollutants and affect the environment due to its hazardous and carcinogenic nature. Thus detoxification of these organic pollutants needs an urgent and effective process.

Several methods have been used but photo-catalytic degradation is one of the superlative and attractive substitutes for the degradation of these organic pollutants. Therefore,  $\text{Sb}_2\text{O}_3$  has been proposed as a catalyst for the detoxification of organic dye in the presence of UV radiation.

Organic solvents are also one of the hot environmental problems and badly effect the environment due to their toxicity. One of these organic solvents is chloroform which cause cardiac or respiratory arrest [18] and depress the central nervous system [19]. Thus it is very important organic compound to have details study and develop devices or sensors for the detection and quantification of chloroform using microstructure materials. In general, metal oxides are being extensively utilized due to their unique surface activities imparted by huge surface areas, which can make them ideal sensing elements as chemi-sensors. The detection of chloroform in liquid phase by I-V technique using antimony oxide surface is developed for the first time.

In the present investigation we have made an attempt to develop a photo-catalyst and chemi-sensor and for this purpose antimony oxide ( $\text{Sb}_2\text{O}_3$ ) microstructures were synthesized.  $\text{Sb}_2\text{O}_3$  microstructures were characterized by UV, FT-IR, Raman spectroscopy, XRD, FE-SEM and EDS. These microstructures were applied for catalytic application and sensing application and demonstrated good degradation and sensing properties.

## 2. Experimental

### 2.1. Materials and Methods

Analytical grade antimony chloride, hexamethylene diamine, ammonium hydroxide, acridine orange, and chloroform were purchased from Sigma-Aldrich and used as received. The solution was made in double distilled water before performing any reaction. For the synthesis of antimony oxide microstructure, the solutions were prepared by adding antimony chloride (0.5 M, 50.0 mL) and hexamethylene diamine (0.5 M, 50 mL) in distill water in equimolecular proportion. The pH (9.3) was adjusted by adding drop wise ammonium hydroxide and then magnetically stirred for 6 hour at 60.0°C. After cooling, white precipitates were obtained and washed with acetone for two to three times and dried at room temperature. The as-grown microstructure antimony oxide does reveal better photo catalytic activity and chemical sensing property. For this purpose, photo-degradation of AO is investigated as model dye compound that results in a better chemical action on antimony oxide microstructure. Chloroform was used as model compound for sensor application. Structural characterizations of the as-grown

materials were investigated using field emission scanning electron microscope (FE-SEM; JSM-7600F, Japan), x-ray diffraction (XRD; X'Pert Explorer, PANalytical diffractometer) data was executed with  $\text{Cu-K}\alpha_1$  radiation. Fourier transforms infrared spectrometer (FT-IR; Perkin Elmer) spectrum was recorded in KBr dispersion in the range of 400 to 4000  $\text{cm}^{-1}$ . UV/visible spectrum were recorded at 291 nm (Perkin Elmer-Lambda 950-UV-visible spectrometer). Raman-scattering spectrum was measured at room temperature with the  $\text{Ar}^+$  laser line as an excitation source. The chemical sensing of  $\text{Sb}_2\text{O}_3$  electrodes have been primarily investigated by I-V technique, where chloroform is used as a target compound. A thin-film was fabricated on electrode substrate by  $\text{Sb}_2\text{O}_3$  micro-materials with conducting binder for fabricating the sensor substrate.

### 2.2. Photo-Catalytic Experiments

Photo-degradation of AO was examined by optical absorption spectroscopy. The catalytic reaction was carried out in a 250.0 mL beaker, which contain 150.0 ml of AO dye solution (0.03 mM) and 150.0 mg of catalyst. Prior to irradiation, the solution was stirred and bubbled with oxygen for at least 15 min in the dark to allow equilibrium of the system so that loss of compound due to the adsorption can be taken into account. The suspension was continuously purged with oxygen bubbling throughout the experiment. Irradiation was carried out using 250W high pressure Mercury lamps. Samples (5.0 ml) were collected before and at regular intervals during the irradiation and acridine orange solution were separated from the photo-catalyst by centrifugation before analysis. The degradation was monitored by measuring the absorbance using UV-visible spectrophotometer (Lambda 950). The absorbance of AO (0.03 mM) was followed at 491.0 nm wavelength.

### 2.3. Fabrication of Gold Electrode Using $\text{Sb}_2\text{O}_3$

Gold electrode (surface area, 0.0216  $\text{cm}^2$ ) is coated with as-grown  $\text{Sb}_2\text{O}_3$  using butyl carbitol acetate (BCA) and ethyl acetate (EA) as a coating agent. Then it is kept in the oven at 60.0°C for 3.0 h until the film is completely dried. 0.1 M phosphate buffer solution at pH 7.0 is made by mixing 0.2 M  $\text{Na}_2\text{HPO}_4$  and 0.2 M  $\text{NaH}_2\text{PO}_4$  solution in 100.0 mL de-ionize water.

### 2.4. Detection of Chloroform Using I-V Technique

A cell is constructed consisting of microstructure coated gold electrode as a working electrode and Pd wire is used as counter electrode. Chloroform solution is diluted at different concentrations in DI water and used as a target

chemical. Amount of 0.1 M phosphate buffer solution was kept constant as 20.0 mL for all measurement. Solution was prepared with various concentrations of chloroform in DI water. The ratio of voltage and current (slope of calibration curve) is used as a measure of chloroform sensitivity. Electrometer is used as a voltage sources for I-V measurement in simple two electrode system.

### 3. Results and Discussion

#### 3.1. UV/Visible Spectroscopy

An optical property is one of the most important properties of any material for evaluation of its photo-catalytic activity. The wavelength ( $\lambda_{\max}$ ) of as-grown  $\text{Sb}_2\text{O}_3$  was measured by using UV/visible spectrometer and presented in **Figure 1**. It displays a well-defined and strong absorption peak at 291.0 nm which is a characteristic absorption peak corresponds to the orthorhombic type of  $\text{Sb}_2\text{O}_3$ . No other peak related with impurities and structural defects were observed in the spectrum which confirms that the synthesized micro-materials contain only crystalline  $\text{Sb}_2\text{O}_3$ . Further band gap energy was calculated on the basis of the maximum absorption band of  $\text{Sb}_2\text{O}_3$  microstructures and found to be 4.26 eV according to Equation (1).

$$E_{bg} = \frac{1240}{\lambda} \quad (\text{eV}) \quad (1)$$

where  $E_{bg}$  is the band-gap energy and  $l$  is the wavelength (nm) of the photo catalyst.

#### 3.2. FT-IR Spectroscopy

The FT-IR spectrum (**Figure 2**) of as-grown  $\text{Sb}_2\text{O}_3$  powder was measured with standard KBr powder by spectrometer. The absorption band at  $546 \text{ cm}^{-1}$  and  $690 \text{ cm}^{-1}$  represent the stretching frequencies (Sb-O) and oxide bridge functional group (O-Sb-O) in  $\text{Sb}_2\text{O}_3$  [20]. The absorption band at  $3450 \text{ cm}^{-1}$  is mainly due to the stretching vibration of  $\text{H}_2\text{O}$  (O-H) on the surface hydroxyl group or absorbed water. The peak at  $1605 \text{ cm}^{-1}$  is observed due to bending vibration of  $\text{H}_2\text{O}$ . The lower intensity of the peak revealed the low contents of moisture in the as-grown sample. The peak at  $1420 \text{ cm}^{-1}$  was assigned to  $\text{CO}_2$  absorbed from the environment.

#### 3.3. Raman Spectroscopy

Raman spectroscopy was used to elucidate the structure of the as-grown product and discriminate from other metal oxides. **Figure 3** shows the Raman spectrum taken using Raman microscope objective at low laser power at room conditions. The main features of the wave-number are observed at about 220, 298, 443, 505, 590, and 685

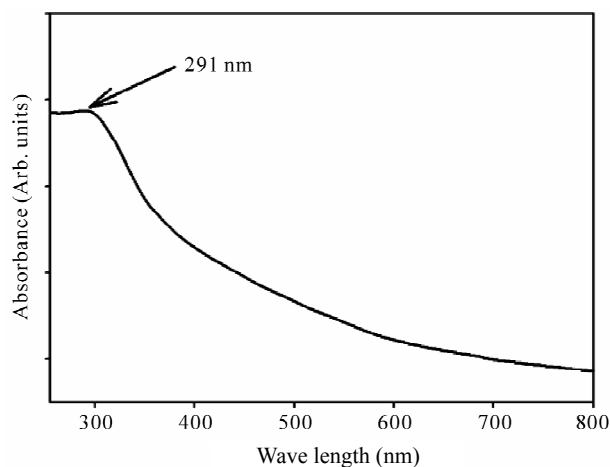


**Figure 1.** UV/visible spectrum of as-grown  $\text{Sb}_2\text{O}_3$  synthesized compound.

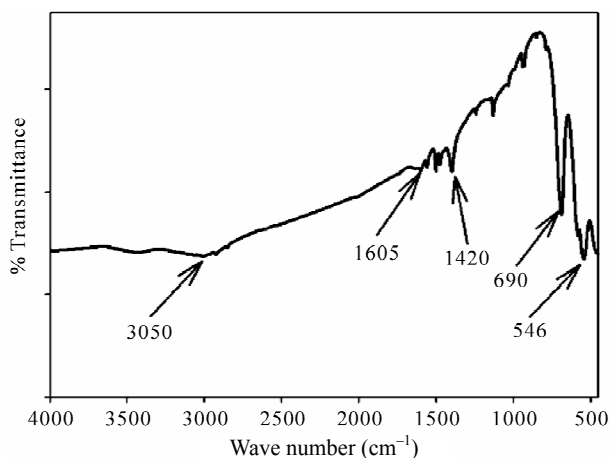


**Figure 2.** FT-IR spectrum of as-grown  $\text{Sb}_2\text{O}_3$  microstructure with standard KBr compound.

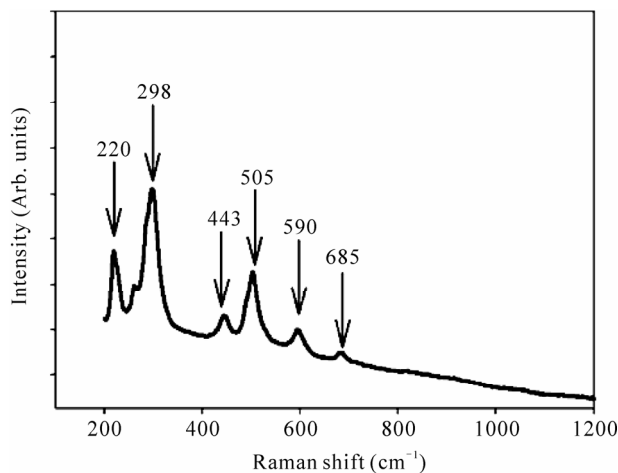


**Figure 3.** Studies of Raman spectroscopy of as-grown  $\text{Sb}_2\text{O}_3$  microstructures.

$\text{cm}^{-1}$  which are responsible for Sb-O stretching vibration [21]. These large bands may be assigned to a magnetite phase of antimony oxide micro-flowers.

### 3.4. XRD Analysis

The crystal phase of the as-grown antimony oxide was investigated by XRD analysis and shown in **Figure 4**. XRD analysis showed diffraction peaks which could be indexed to (110), (111), (121), (131), (002), (112), (211), (221), (002), (240), (052), (161), (113), (133), (072), (341), and (312) phases, which revealed the existence of well-crystalline orthorhombic type of  $\text{Sb}_2\text{O}_3$ . The diffraction pattern of the as-prepared sample matches JCPDS # 74-1725. The diffraction peaks showed that the antimony oxide produced different crystalline phase [22,23]. X-ray diffraction thus confirmed that the obtained microstructure is well-crystalline orthorhombic type of  $\text{Sb}_2\text{O}_3$ .

### 3.5. Measurement of FE-SEM & EDS

Morphology of the microstructure was investigated by FE-SEM and shown in **Figure 5**. High and low magnification of FESEM images [**Figures 5(a-c)**] showed flower shape structure in micro-level for the as-grown products. The EDS spectrum corroborated the composition of  $\text{Sb}_2\text{O}_3$ , which is presented in the **Figure 5(d)**. The EDS spectra indicate that the as-grown microstructure is composed of Sb and O. No other peak related to elements

other than Sb and O were detected. The atomic percent of Sb and O were determined in the as-grown microstructure as 42.76% and 57.24%, respectively.

## 4. Applications

### 4.1. Photo-Catalytic Degradation

**Figure 6(a)** exhibits the change in absorption spectra for the photo-catalytic degradation of AO dye as a function of irradiation time. It is found that irradiation of aqueous suspension of AO dye in the presence of  $\text{Sb}_2\text{O}_3$  microstructure leads to decrease in absorption intensity. It can be seen that the maximum absorbance at 491.0 nm gradually decreases with increase in irradiation time. **Figure 6(b)** shows the change in absorbance as a function of irradiation time for the dye derivative in the absence and presence of  $\text{Sb}_2\text{O}_3$  microstructure. Irradiation of an aqueous solution of AO in the presence of synthesized microstructure leads to decrease in absorption intensity. **Figure 6(c)** shows a plot for the percent degradation vs irradiation time (min) for the oxygen saturated aqueous suspension of acridine orange (AO) in the presence and absence the synthesized metal oxide microstructures. It could be seen from the figure that 63.0% (in the presence of  $\text{Sb}_2\text{O}_3$  microstructure) of the compound degraded after 150.0 minutes of irradiation time whereas in the absence of photo-catalyst no observable loss of dye

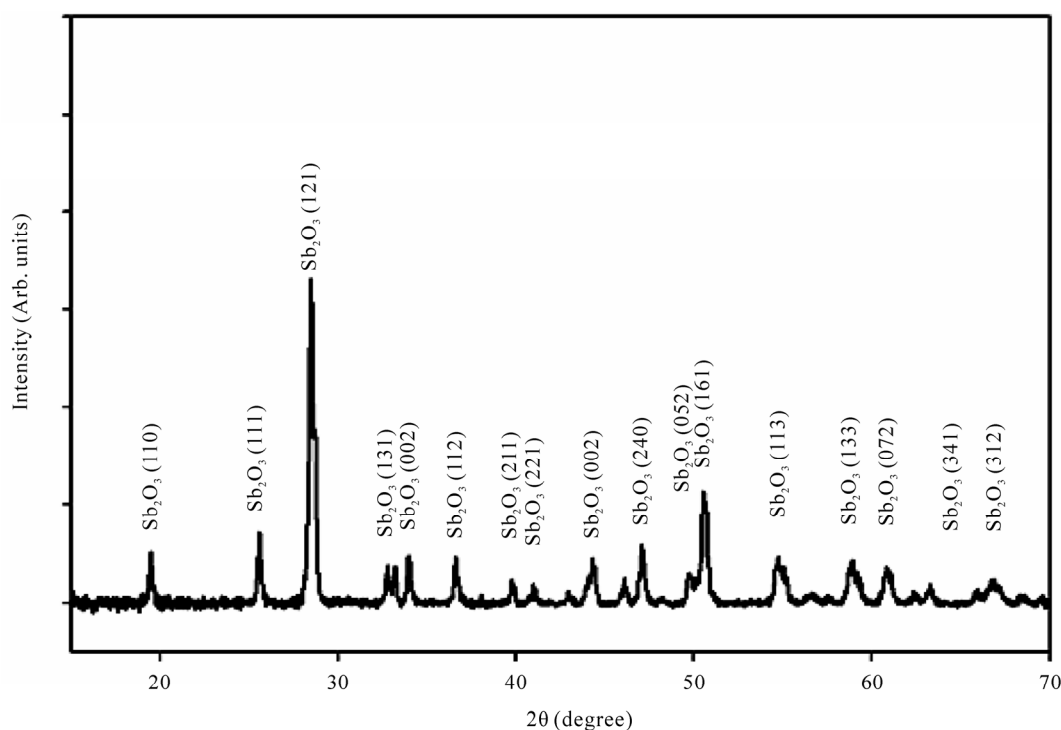


**Figure 4.** XRD pattern of as-grown synthesized  $\text{Sb}_2\text{O}_3$  microstructures.

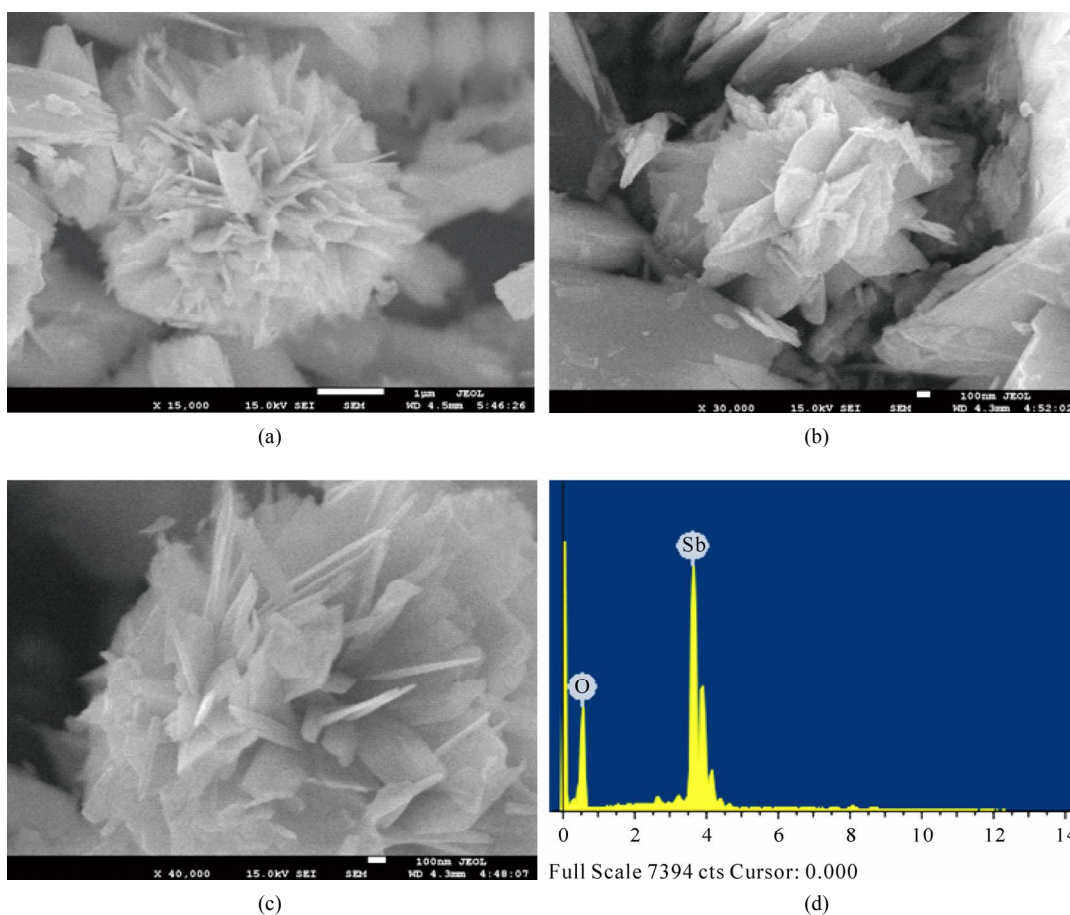


Figure 5. The FE-SEM morphology of as-grown  $\text{Sb}_2\text{O}_3$ . (a) to (c) low to high magnified images and (d) is EDS spectrum of as grown antimony-oxide powder.

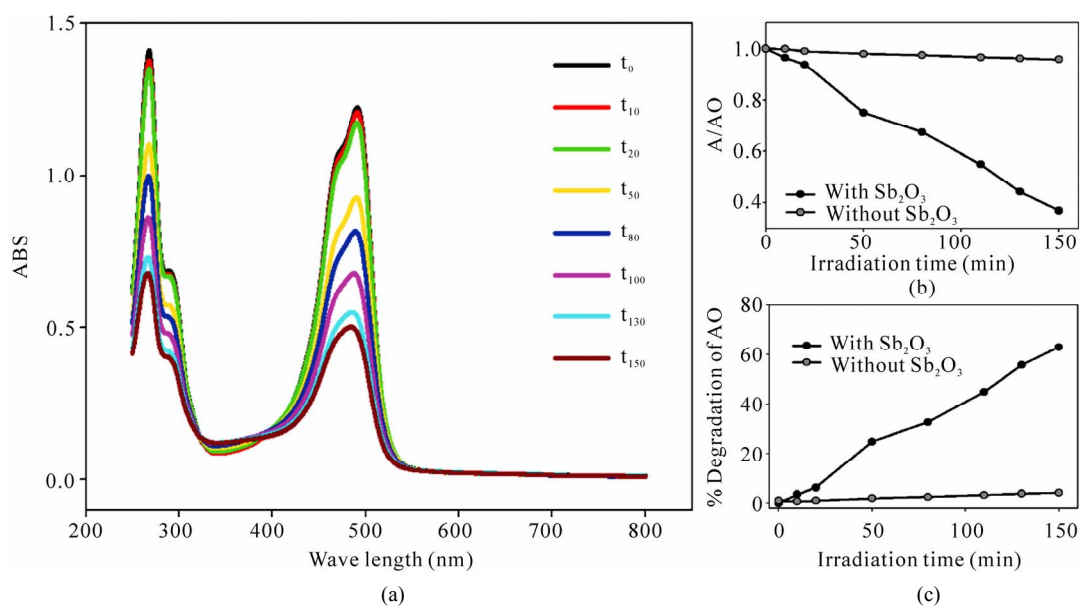
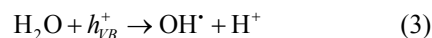
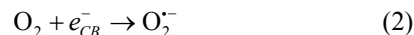
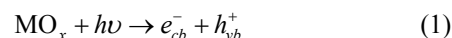


Figure 6. Photo-catalytic degradation of AO using mf- $\text{Sb}_2\text{O}_3$ . (a) Spectrum of AO at different time interval; (b) Comparison of absorbance and (c) % degradation in different time intervals of AO in presence and absence of as-grown mf- $\text{Sb}_2\text{O}_3$ .

could be seen. Above results clearly indicate that prepared microstructure showing considerable photo catalytic activity has very simple synthesis procedure and low cost, so it can also be used as a photo catalyst beside other metal oxide.

Antimony oxide is one of the promising semiconductors due to their various morphological (micro-flower shape) and chemical properties, availability, easy to use, easy to synthesis, less toxic, lower cost, higher surfaces area, and high absorption of light quanta. Mechanism of heterogeneous photo catalysis has been discussed extensively in literature. Briefly when metal oxide absorb energy which is more than its band gap energy it results in the generation of electron and hole pairs with free electrons produced in the empty conduction band ( $e_{CB}^-$ ) leaving behind an electron vacancy or "hole" in the valence band ( $h_{VB}^+$ ). During this photo catalytic activity, the electron and hole may migrate to the catalyst surface where they participate in redox reactions. Specially,  $h_{VB}^+$  may react with surface-bound  $H_2O$  or  $OH^-$  to produce the hydroxyl radical and  $e_{CB}^-$  is picked up by oxygen to

generate superoxide radical anion [24-26] as mentioned in the Equation (1)-(3).



The hydroxyl radicals ( $OH^{\cdot}$ ) and superoxide radical anions ( $O_2^{\cdot-}$ ) are shows as a primary oxidizing species in the photo catalytic processes and contribute to the oxidation process by attacking the dye molecules and would results in the bleaching of the AO dye.

#### 4.2. Chloroform Detection

The as-grown flower-shape  $Sb_2O_3$  was employed for the detection of chloroform in solution phase. Pd and gold electrodes are used as counter electrode and working electrode respectively. I-V technique is followed to measure the changing of current in each injection of chemical solution in the 20.0 mL phosphate buffer solu-

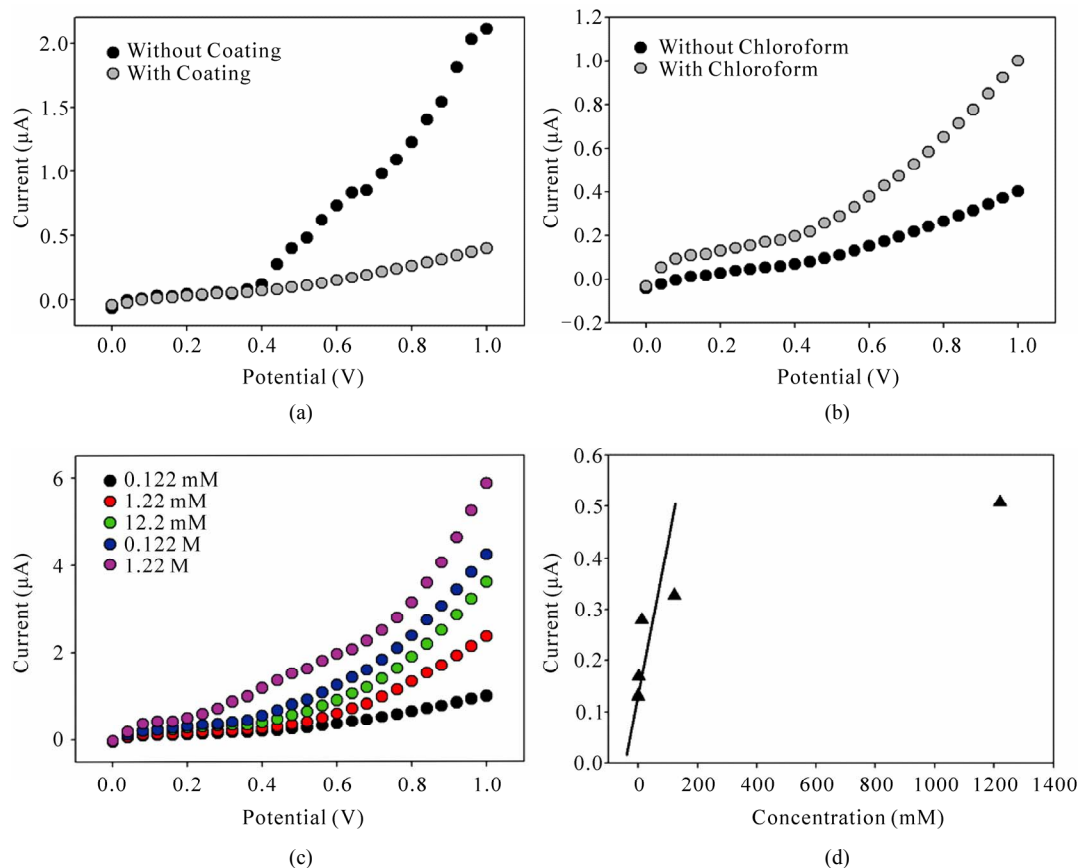


**Figure 7.** I-V characterization of as-grown  $Sb_2O_3$  microstructures. (a) Comparison of with and without coating surface; (b) Comparison of with and without chloroform sample injection; (c) Concentration variation of chloroform and (d) calibration plot.

tion. The chloroform was used as a detecting chemical in the liquid phase as a chemical sensor [25,26]. The sensing characteristics of I-V sensors (two electrodes system) having  $\text{Sb}_2\text{O}_3$  thin film has been studied, which is presented in the **Figure 7**. I-V responses sensor having  $\text{Sb}_2\text{O}_3$  thin film as a function of time for the chloroform is shown in **Figures 7(a)** and **(b)**. The time delaying for electrometer was kept 1.0 sec. The concentration of chloroform was varied from 0.122 mM to 12.2 M by adding de-ionized water in different proportions. A significant increase in the current value with applied potential is clearly demonstrated. The gray-solid and dark-solid dotted curves indicate the response of the film before and after injecting 100.0  $\mu\text{L}$  chemicals in bulk solution. Significant increase in the sample current is measured after injection of target component. 0.122 mM concentration of chloroform was initially taken in the cell and added the higher concentration (each step, 10 times) is in each injection from the stock concentration of chloroform, which was added to the 20 mL bulk buffer solution. Each I-V response to varying concentration of chemicals from 0.122 mM to 12.2 M on thin micro-flower  $\text{Sb}_2\text{O}_3$  coatings for 10s (delay of time) was presented in the **Figure 7(c)**. It shows current of  $\text{Sb}_2\text{O}_3$  as a function of target concentration at room temperature. It is observed that at lower to higher concentration of target compound, the current increases gradually. A wide range of chloroform concentration was chosen to study the possible detection limit, which is examined in 0.122 mM to 1.22 M. The calibration curve was plotted from the variation of chloroform concentration, which is shown in the **Figure 7(d)**. The sensitivity is calculated from the calibration curve, which is closed to  $0.1154 \mu\text{A}\cdot\text{cm}^{-2}\cdot\text{mM}^{-1}$ . The linear dynamic range of this sensor exhibits from 0.122 mM to 1.22 M with linearity ( $R = 0.7898$ ) in short response time (10.0 s) and the detection limit was found 0.1 mM (3N/S).

## 5. Conclusions

The micro-flower shaped  $\text{Sb}_2\text{O}_3$  has been successfully synthesized using  $\text{SbCl}_3$  and HMDA by direct thermal stirrer technique in the alkaline medium. The composition and detail structural characterization have been studied by UV, FT-IR, Raman spectroscopy, XRD, FE-SEM, and EDS which revealed that the synthesized microstructures are well-crystalline, possessing orthorhombic type of  $\text{Sb}_2\text{O}_3$ . The potential applications on catalytic behavior and chemical sensing were carried out with as-grown micro-flower  $\text{Sb}_2\text{O}_3$  materials. The photo catalytic performance of  $\text{Sb}_2\text{O}_3$  materials were evaluated by degradation of AO which efficiently degraded the dye. By applying to the detection and quantification of chloroform,

the performance of the developed chloroform sensor is excellent in terms of sensitivity, detection limit, linear dynamic ranges, and response time.

## 6. Acknowledgements

Authors are thanks full for financial support to the deanship of scientific research, Najran University, Najran, Saudi Arabia.

## REFERENCES

- [1] K. Ozawa, Y. Sakka and A. Amamo, "Preparation and Electrical Conductivity of Three Types of Antimonic Acid Films," *Journal of Materials Research*, Vol. 13. No. 4, 1998, pp. 830-833. doi:10.1557/JMR.1998.0107
- [2] K. S. Liu, J. Zhai and L. Jiang, "Fabrication and Characterization of Superhydrophobic  $\text{Sb}_2\text{O}_3$  Films," *Nanotechnology*, Vol. 19, No. 16, 2008, p. 165604. doi:10.1088/0957-4484/19/16/165604
- [3] Z. T. Deng, D. Chen, F. Q. Tang, X. W. Meng, J. Ren and L. Zhang, "Orientated Attachment Assisted Self-Assembly of  $\text{Sb}_2\text{O}_3$  Nanorods and Nanowires: End-to-End Versus Side-by-Side," *Journal of Physical Chemistry*, Vol. 111, No. 14, 2007, pp. 5325-5330.
- [4] Y. X. Zhang, G. H. Li and L. D. Zhang, "Growth of  $\text{Sb}_2\text{O}_3$  Nanotubes via a Simple Surfactant-Assisted Solvothermal Process," *Chemistry Letters*, Vol. 33, No. 3, 2004, pp. 334-335. doi:10.1246/cl.2004.334
- [5] S. B. Khan, M. Faisal, M. M. Rahman and A. Jamal, "Low-temperature Growth of ZnO Nanoparticles: Photocatalyst and Acetone Sensors," *Talanta*, March 2011.
- [6] M. Faisal, S. B. Khan, M. M. Rahman, A. Jamal and A. Umar, "Ethanol Chemi-Sensor: Evaluation of Structural, Optical and Sensing Properties of CuO Nanosheets," *Materials Letters*, Vol. 65, No. 9, 2001, pp. 1400-1403. doi:10.1016/j.matlet.2011.02.013
- [7] B. J. Li, Y. B. Zhao, X. M. Xu, C. L. Zhang, Z. S. Wu and Z. J. Zhang, "Fabrication of Hollow  $\text{Sb}_2\text{O}_3$  Microspheres by PEG Coil Template," *Chemistry Letters*, Vol. 35, No. 9, 2006, p. 1026. doi:10.1246/cl.2006.1026
- [8] C. Ye, G. Meng, L. Zhang, G. Wang and Y. Wang, "A Facile Vapor-Solid Synthetic Route to  $\text{Sb}_2\text{O}_3$  Fibrils and Tubules," *Chemical Physics Letters*, Vol. 363, No. 1-2, 2002, pp. 34-38. doi:10.1016/S0009-2614(02)01018-7
- [9] A. Umar, M. M. Rahman and Y. B. Hahn, "MgO Polyhedral Nanocages and Nanocrystals Based Glucose Biosensor," *Electrochemistry Communications*, Vol. 11, No. 7, 2009, pp. 1353-1357. doi:10.1016/j.elecom.2009.04.033
- [10] M. M. Rahman, A. Jamal, S. B. Khan and M. Faisal, "Characterization and Applications of as Grown  $\beta\text{-Fe}_2\text{O}_3$  Nanoparticles Prepared by Hydrothermal Method," *Journal of Nanoparticle Research*, 2011. doi:10.1007/s11051-011-0301-7
- [11] R. W. Siegel, "Nanostructured Materials—Mind over Matter," *Nanostructured Materials*, Vol. 4, No.1, 1994,

- pp. 121-138. doi:10.1016/0965-9773(94)90134-1
- [12] A. Umar, M. M. Rahman, A. Al-Hajry and Y. B. Hahn. "Highly-Sensitive Cholesterol Biosensor Based on Well-Crystallized Flower-Shaped ZnO Nanostructures," *Talanta*, Vol. 78, No. 1, 2009, pp.284-289. doi:10.1016/j.talanta.2008.11.018
- [13] P. Liu, Y.H. Zhang, M. W. Zhang, W. H. Zhang and Y. T. Qian, "Preparation of Nanocrystalline Antimony Oxide Powders by Use of  $\gamma$ -Ray Radiation—Oxidization Route," *Materials Science and Engineering B*, Vol. 49, No. 1, 1997, pp. 42-45. doi:10.1016/S0921-5107(97)00065-2
- [14] C. G. Granqvist and R. A. Buhmann, "Ultrafine Metal Particles," *Journal of Applied Physics*, Vol. 47, No. 5, 1976, pp. 2200-2219. doi:10.1063/1.322870
- [15] Z. L. Zhang, L. Guo and W. D. Wang, "Synthesis and Characterization of Antimony Oxide Nanoparticles," *Journal of materials Research*, Vol. 16, No. 3, 2001, pp. 803-805. doi:10.1557/JMR.2001.0096
- [16] M. Faisal, M. A. Tariq and M. Muneer, "Photocatalysed Degradation of Two Selected Dyes in UV-Irradiated Aqueous Suspensions of Titania," *Dyes Pigments*, Vol. 72, No. 2, 2007, pp. 233-239. doi:10.1016/j.dyepig.2005.08.020
- [17] S. B. Khan, M. Faisal, M. M. Rahman and A. Jamal, "Exploration of CeO<sub>2</sub> Nanoparticles as a Chemi-Sensor and Photo-Catalyst for Environmental Applications," *Science of the Total Environment*, Vol. 409, No. 15, 2011, pp. 2987-2992. doi:10.1016/j.scitotenv.2011.04.019
- [18] A. Umar, M. M. Rahman, A. Al-Hajry and Y.-B. Hahn. "Enzymatic Glucose Biosensor Based on Flower-Shaped Copper Oxide Nanostructures Composed of Thin Nanosheets," *Electrochemistry Communications*, Vol. 11, No. 2, 2009, pp. 278-281. doi:10.1016/j.elecom.2008.11.027
- [19] M. M. Rahman, A. Umar and K. Sawada. "Development of Amperometric Glucose Biosensor Based on Glucose Oxidase Co-Immobilized with Multi-Walled Carbon Nanotubes at Low Potential." *Sensors and Actuators B: Chemical*, Vol. 137, No. 1, 2009, pp. 327-333. doi:10.1016/j.snb.2008.10.060
- [20] I. O. Mazali, W. C. Las and M. Cilense, "Synthesis and Characterization of Antimony Tartrate for Ceramic Precursors," *Journal of Materials Synthesis and Processing*, Vol. 7, No. 6, 1999, pp. 387-391. doi:10.1023/A:1021822115116
- [21] Z. Deng, D. Chen, F. Tang, J. Ren and A. J. Muscat, "Synthesis and Purple-Blue Emission of Antimony Trioxide Single-Crystalline Nanobelts with Elliptical Cross Section," *Nano Research*, Vol. 2, No. 2, 2009, pp. 151-160. doi:10.1007/s12274-009-9014-y
- [22] D. Wang, Y. Zhou, C. Song and M. Shao, "Phase and Morphology Controllable Synthesis of Sb<sub>2</sub>O<sub>3</sub> Microcrystals," *Journal of Crystal Growth*, Vol. 311, No. 15, 2009, pp. 3948-3953. doi:10.1016/j.jcrysgro.2009.06.020
- [23] Y. Hu, H. Zhang and H. Yang, "Direct Synthesis of Sb<sub>2</sub>O<sub>3</sub> Nanoparticles via Hydrolysis-Precipitation Method," *Journal of Alloys and Compounds*, Vol. 428, No. 1-2, 2007, pp. 327-331. doi:10.1016/j.jallcom.2006.03.057
- [24] B. S. Naidu, M. Pandey, V. Sudarsan, R. K. Vatsa and R. Tewari, "Photoluminescence and Raman Spectroscopic Investigations of Morphology Assisted Effects in Sb<sub>2</sub>O<sub>3</sub>," *Chemical Physics Letters*, Vol. 474, No. 1-3, 2009, pp. 180-184. doi:10.1016/j.cplett.2009.04.050
- [25] M. A. Tariq, M. Faisal and M. Muneer, "Semiconductor-Mediated Photocatalysed Degradation of Two Selected Azo Dye Derivatives, Amaranth and Bismarck Brown in Aqueous Suspension," *Journal of Hazardous Materials*, Vol. 127, No. 1-3, 2005, pp.172-179. doi:10.1016/j.jhazmat.2005.07.001
- [26] M. Faisal, S.B. Khan, M.M. Rahman and A. Jamal, "Role of ZnO-CeO<sub>2</sub> Nanostructures as a Photocatalyst and Chemi-Sensor," *Journal of Materials Sciences & Technology*, 2011 (In press).